Metalurgi (2021) 1: 25 - 32

LIPI

METALURGI
Majalah Ilmu dan Teknologi
p-ISSN 0126-3188 | e-ISSN 2443-3926
www.ejurnalmaterialmetalurgi.com

STUDY ON MICROSTRUCTURE AND MECHANICAL PROPERTIES OF Mg-Zn-Fe-Cu-Co AS HIGH ENTROPY ALLOYS FOR URETERAL IMPLANT

Andi Mulya Ashari 1[a,*], Franciska Pramuji Lestari[b], Rahma Nisa Hakim[b], Inti Mulyati[b], Yudi Nugraha Thaha[b], Ika Kartika[b], Eddy Agus Basuki[a]

[a] Departement of Metallurgical Engineering, Bandung Institute of Technology
Jl. Ganesha No. 10, Bandung, Indonesia 40132
[b] Research center for Metallurgy and Material, Indonesian Institute of Science
Gedung 470, Kawasan PUSPIPTEK Serpong, Tangerang Selatan, Indonesia 15343
*E-mail: andimulyaa94@gmail.com

Masuk tanggal : 12-03-2021, revisi tanggal : 09-04-2021, diterima untuk diterbitkan tanggal 30-04-2021

Abstrak

Magnesium dan paduannya merupakan kandidat yang menjanjikan untuk bahan yang dapat terdegradasi dengan sifat biokompatibilitas yang baik. Paduan berdasarkan komposisi Mg-Zn-Fe-Cu-Co dirancang dengan metode equiatomic paduan entropi tinggi. Makalah ini membahas struktur mikro dan sifat mekanik dari paduan entropi tinggi. Serbuk Mg (60 µm), Zn (45 µm), Fe (10 µm), Cu (63 µm), dan Co (1 µm) dicampur dan digiling menggunakan shaker mill pada 700 rpm selama 30 menit di atmosfer udara pada temperatur kamar. Serbuk logam hasil gilingan yang dihasilkan dipadatkan dan disinter pada tekanan 300 MPa selama 180 detik dan 600 MPa selama 120 detik. Sintering dilakukan pada suhu 700 °C selama 2 jam dalam tungku vakum dengan laju pemanasan 5 °C / menit pada kondisi atmosfer argon dengan kemurnian tinggi. Pengaruh variasi kandungan magnesium terhadap struktur mikro dan sifat mekanik paduan Mg-Zn-Fe-Cu-Co dilakukan dengan SEM-EDS (*scanning electron microscope-energy dispersive spectroscopy*), XRD (*x-ray diffraction*) dan uji keras secara mikro. Paduannya pada dasarnya multifase dan kristal. Paduan 20Mg-20Zn-20Fe-20Cu-20Co terdiri dari fase HCP (*hexagonal closed packed*) dan fase kubik. Sifat fisik dan mekanik Mg-Zn-Fe-Cu-Co dipengaruhi oleh kandungan magnesium dalam paduan matriks. Adanya pori-pori mengindikasikan pemadatan dan proses sintering yang belum tuntas. Paduan memiliki kekerasan sedang antara 286,06 HV - 80,98 HV, sedangkan densitas paduan relatif sedang pada kisaran 3,057 g.cm^{-3} sampai 1,71 g.cm^{-3}. Larutan padat dan penguatan presipitasi intermetalik diyakini sebagai mekanisme penguatan utama paduan. Disimpulkan bahwa entropi tinggi adalah metode yang menjanjikan untuk pemrosesan paduan Mg. Paduan dengan komposisi kimia 20Mg-20Zn-20Fe-20Cu-20Co memiliki sifat mekanik optimal yang memenuhi persyaratan minimum paduan entropi tinggi sebagai kandidat aplikasi implan ureter.

Kata Kunci: Logam mampu luruh, paduan entropi tinggi, metalurgi serbuk, paduan Mg-Zn-Fe-Cu-Co

Abstract

Magnesium and its alloys are promising candidates for degradable materials with good biocompatibility. Alloys based on Mg-Zn-Fe-Cu-Co compositions were designed using the equiatomic method of high entropy alloy. This paper discusses the microstructure and mechanical properties of these new high entropy alloys. Pure Magnesium (60 µm), Zinc (45 µm), Fe (10 µm), Cu (63 µm), and Co (1 µm) powder were mixed and milled using a shaker mill at 700 rpm for 30 minutes in an air atmosphere at room temperature. The resulting milled powders were compacted and sintered at 300 MPa for 180 s and 600 MPa for 120 s. Sintering was performed at 700 ºC for 2 hours in a tube vacuum furnace at a 5 °C/min heating rate under a high purity argon atmosphere. The effect of variations in magnesium content on the microstructure (SEM-EDS and XRD) and mechanical properties (microhardness tester) of the Mg-Zn-Fe-Cu-Co alloy were performed. The alloys were multiphase and crystalline. The 20Mg-20Zn-20Fe-20Cu-20Co alloy consisted of the HCP (hexagonal closed packed) phase and cubic phase. The physical and mechanical properties of Mg-Zn-Fe-Cu-Co were affected by the magnesium content in the matrix alloys. The presence of pores indicated uncomplete compaction and sintering process. The alloys have a medium hardness of between 286.06 HV - 80.98 HV, while the densities of the alloys were relatively moderate in the range of 3.057 g.cm^{-3} to 1.71 g.cm^{-3}. Solid solution and intermetallic precipitation strengthening were believed the primary strengthening mechanics of the alloys. It is concluded that high entropy is a promising method for the processing of

Mg alloys. Alloy with the chemical composition of 20Mg-20Zn-20Fe-20Cu-20Co had optimal mechanical properties that meet the minimum requirements of high entropy alloys as a candidate for ureteral implant applications.

Keywords: *Biodegradable metal, high entropy alloy, powder metallurgy, Mg-Zn-Fe-Cu-Co alloy*

1. INTRODUCTION

Urinary tract stones (UTI) or kidney stones are a disease that affects the urinary system. Urinary tract infections are frightening and remain a major health burden of working age. In Indonesia, the prevalence of urinary tract infection patients per 1,000 Indonesian populations is 0.6% or 6% [1]. The ureteral lesion-induced bacterial infection, hydronephrosis, urinary cysts, and other urinary system complications, that affected the patient's life quality [2]. These diseases bring tremendous physical pain and heavy economic burden to a patient [3]-[4]. After surgery, the ureteral lesion healed with a ureteral stent, that placed in the urinary tract to keep urine flowing smoothly and prevent ureteral stenosis [2],[5]. However, the ureteral stent is an extraneous body for a sufferer, there have been many problems surrounding the use of ureteral stent, as well as stent fractures, encrustations establishment, urethral re-formations, and obstructions. The good ureteral stent has the following advantages: (1) good mechanical and drainage properties; (2) good biocompatibility; (3) X-ray and B-ultrasound radiopaque should be performed regularly after stent implantations [6]. Usually, a conventional ureteral stent is made by the polymer, which is cheap and well-tolerated by the sufferer but was prone and weak, that is not ideal for drainage and support in the ureter [2],[6]. Several studies have reported the use of biodegradable polymers for urethral stents, such as PLA (polylactic acid) [6], PGA (polyglycolide) [7], PCL (polycaprolactone) [2], Poly(L-lactide-co-ε-caprolactone) (PCLC) [8], and their copolymers. In contrast, biodegradable metal stents are of increasing interest in recent times because the mechanical properties of metals are inherently better than polymers and more desirable for stent expansion. The metallic stent is generally applied to treat cardiovascular disease, diseases of the bile duct and digestive tract in 1972 [6]-[5]. Magnesium and its alloys are promising candidates for degradable materials with high strength, low modulus of elasticity, and good biocompatibility [2],[4]-[5],[9]. So far, there have been a few studies on the use of biodegradable metal ureteral stents. In 2017, Zhang [2],[10]-[11] demonstrated that pure Mg, Mg-6Zn (Mass %), and ZK60 alloy have no obvious adverse effects on rat bladders and ZK60 alloy has good mechanical properties, with a uniform elongation of 10-30% and an ultimate tensile strength of 200-400 MPa, making it suitable for use as an implant material. A more recent study by Tie et. al., [5][12] demonstrated pure Mg, Mg-Y, AZ30, and Mg-Zn-Sr alloys have the potential alloys for urological applications.

Alloys are one of the most effective ways to improve the mechanical properties of metals [9],[13]-[16]. As we all know, solid solution strengthening and second phase strengthening are the two main methods to improve the mechanical properties of magnesium alloys [17]-[18]. In 2004, the two research groups respectively released the alloy development strategy of equal atomic ratio and high mixing entropy. They found that high-entropy alloys have a simple microstructure with less than 3 phases, and a cubic solution is the main phase [19]-[20]. Other researchers have studied the mechanical properties of high-entropy alloys [17],[19],[21]. In recent years, extensive and in-depth research has been conducted on the mechanical properties of high-entropy alloys. The composition of high-entropy alloys is mainly concentrated on Fe, Co, Cr, Ni, Ti, V, Cu, and Al [19]. However, there are a few reports on other ingredients such as magnesium, and zinc. The mentioned high entropy alloys usually attain excessive hardness and strength. So it's essential to study Mg-containing high entropy alloys. 20Mg-20Zn-20Fe-20Cu-20Co, 50Mg-25Zn-24Fe-0.5Cu-0.5Co, 70Mg-25Zn-4Fe-0.5Cu-0.5Co, 90Mg-5Zn-4Fe-0.5Cu-0.5Co, and pure Mg had been designed to examine the microstructure and mechanical properties of Mg-containing high entropy alloys in this paper.

2. MATERIALS AND METHODS

2.1. Samples Preparation

Pure elements of Magnesium (60 μm), Zinc (45 μm), Fe (10 μm), Cu (63 μm), and Co (1 μm) powder were weighted on a digital weighing balance in a normal atmosphere, at room temperature. 20Mg-20Zn-20Fe-20Cu-20Co, 50Mg-25Zn-24Fe-0.5Cu-0.5Co, 70Mg-25Zn-4Fe-0.5Cu-0.5Co, 90Mg-5Zn-4Fe-0.5Cu-0.5Co and pure Mg powder mixtures were filled in an alumina jar and mixed using shaker mill machine without ball at 700 rpm for 30 minutes [22]. The mixed powder was then compacted at 300 MPa for 180s and 600 MPa for 120 s under

normal atmospheric, at room temperature. The as-compacted samples were sintered at 700 °C for 2 hours in a tube furnace at 5 °C/min purged with a high purity argon atmosphere during sintering and cooling.

2.2. Test Methods

High entropy alloys have several parameters such as ΔS_{mix}, ΔH_{mix}, ΔG_{mix} (Ω), and atomic size (δ). Following Boltzmann's theory [19]. the mixing entropy for a five-element regular solution is given as:

$$\Delta S_{mix} = -R \sum_{i=1}^{n} C_i \ln C_i \text{ [19][21]} \qquad (1)$$

where C_i is mole percent of a component, and R (8.314 J K^{-1} mol^{-1}) is gas constanta. The mixing enthalpy alloy (ΔHmix) must be between -11.6 and 3.2 kJ / mol [18],[21], to be calculated using the derivative formula in equation 2 of Miedema's macroscopic model [23];

$$\Delta H_{mix} = \sum C_i C_j H_{ij} \text{ [21]} \qquad (2)$$

ΔH_{ij} is the binary enthalpy of the formation of elements i and j. The next criterion is the atomic radius value (δ), stating that the phases which contain mostly solid and intermetallic solutions are formed at values lower than (<) 6.6%, and at values lower than 4% only solid solutions are formed [18]. To calculate the value of δ, this equation 3 is used;

$$\delta = 100 \sqrt{\sum_{i=1}^{n} C_i \left(1 - \frac{r_i}{r}\right)^2} \text{ [21]} \qquad (3)$$

C_i and r_i are the compositions and the atomic radii of elements, i and r are the average atomic radii. Other thermodynamic parameters for predicting the formation of solid solutions are as follows equation 4;

$$\Omega = \frac{Tm\Delta S_{mix}}{\Delta H_{mix}} \text{ [21]} \qquad (4)$$

If $\Omega > 1.1$ and $\delta < 3.6\%$, only a solid solution is formed. If $1.1 < \Omega < 10$ and $3.6\% < \delta < 6.6\%$, only solid solutions and intermetallic compounds are formed, and if $\Omega > 10$ only solid solutions are formed.

The densities and hardness of alloy samples were tested by Archimedes principle according to ASTM B962-17 standard and microhardness Vickers tester. The relative density of respective samples was then calculated by dividing apparent density by theoretical density of the corresponding samples as obtained from the rule of mixture. The same procedure was replicated for 20Mg-20Zn-20Fe-20Cu-20C0, 50Mg-25Zn-24Fe-0.5Cu-0.5Co, 70Mg-25Zn-4Fe-0.5Cu-0.5Co, 90Mg-5Zn-4Fe-0.5Cu-0.5Co and pure Mg serving as control. Micro-hardness Vickers property testing of as-sintered samples was performed using ASTM-E384-17 standard at a load of 0.3 KN for 12 s. The average hardness value obtained from five indents on each sample was recorded as the hardness of each sample. The morphologies of alloys were examined by a JEOL JSM-6390A SEM (scanning electron microscope). The microstructures of sintered samples were characterized by a Rigaku Smartlab diffraction with Co K α radiation (λ = 1.78896A) and scan speed 4 deg/s.

3. RESULTS AND DISCUSSIONS

3.1. Microstructure of Mg-Zn-Fe-Cu-CoAlloys

The thermal analysis results were shown in Fig 1. 20Mg-20Zn-20Fe-20Cu-20Co was melted at about 600 °C and the other alloys were melted at about 650 – 750 °C as seen in Fig 1(b) of DSC curves. Small peaks were shown at a temperature of 425 °C except for 90Mg-5Zn-4Fe-0.5Cu-0.5Co alloy, indicating the formation of the Co-Fe phase [24]. Meanwhile, the valley peak was formed between 500-600 °C, indicating the formation of the $MgZn_2$ phase [25]. Also, the XRD results were matched with the thermal analysis results. According to the TGA results in Fig 1(b), it is shown a difference between 20Mg-20Zn-20Fe-20Cu-20Co alloy and other alloys at a temperature of 400 °C. This was caused by Mg oxidation which changes the mass in the alloy.

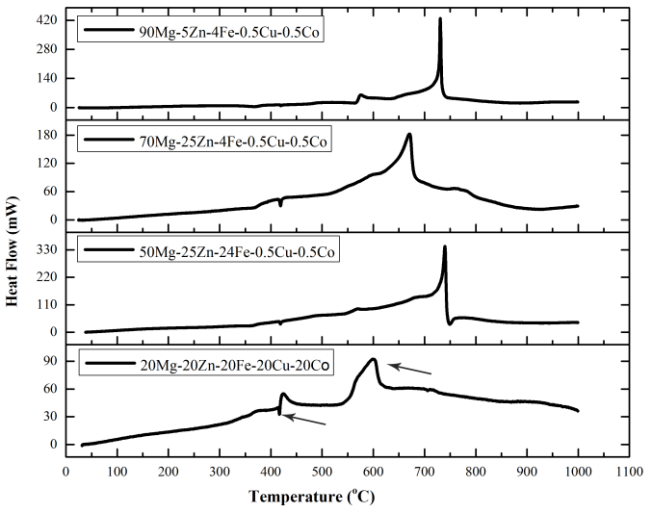

(a)

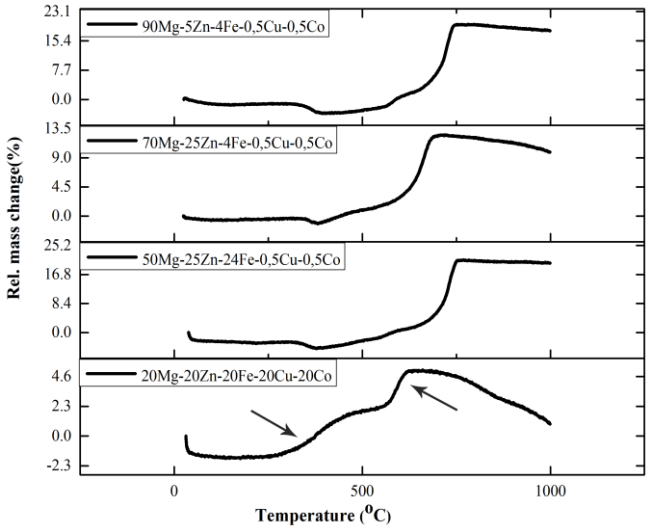

(b)

Figure 1. (a) DSC result and (b) TG result of Mg-Zn-Fe-Cu-Co alloy

The XRD (x-ray diffraction) patterns were shown in Fig 2. Based on equation (1), when the alloys have the same atomic ratio, the mixing entropy reached the maximum. Therefore, as the Mg atomic percentage increases, the mixing entropy decreased [19]. Table 1 shows the entropy results. It is seen that the effect of high mixing entropy significantly occurs in 20Mg-20Zn-20Fe-20Cu-20Co alloy. The solid solution phase was formed previously to the complex intermetallic phase. Only Mg and Co-Fe phase with the structure of HCP and cubic was found in 20Mg-20Zn-20Fe-20Cu-20Co. Other alloys only form complex intermetallic phases, such as the $MgZn_2$ phase, except 90Mg-5Zn-4Fe-0.5Cu-0.5Co which forms the Mg solid solution phase. Moreover, it is shown that the alloys of 50Mg-25Zn-24Fe-0.5Cu-0.5Co and 70Mg-25Zn-4Fe-0.5Cu-0.5Co forms $MgZn_2$, Cu_2Zn, MgO, αMg, and Fe phases.

The $MgZn_2$ phase was formed due to the excess Zn element in Mg. The $MgZn_2$ phase is very easy to form because an $MgZn_2$ phase is more stable than Zn which dissolves in the Mg alloy [25]. Based on equations 2 and 3, there is a relationship between enthalpy and δ. The value of δ increases as the enthalpy value decreases [26]-[27]. Thus, the HEA alloy will form a metallic glass alloy with an unstable structure [26],[28]. In this case, the 50 Mg and 70 Mg alloys are characterized by the predominant formation of the intermetallic phase.

The SEM (scanning electron microscope) images of as-sintered Mg-Zn-Fe-Cu-Co alloys were shown in Fig 3.

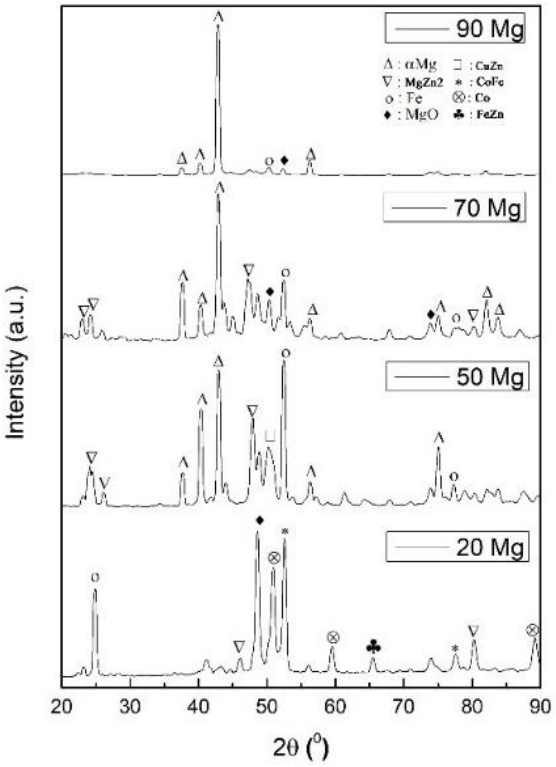

Figure 2. XRD patterns of Mg-Zn-Fe-Cu-Co alloys

The grey globular structure was distributed dispersedly in the base phase of 20Mg-20Zn-20Fe-20Cu-20Co alloy, which was indicated to be the Co-Fe phase. The XRD results match with those of the EDS (energy dispersive spectroscopy) mapping shown in Fig 3. The widths of the globular structure were found less than 5 μm. While, the base phase was a solid solution, which was made up of Mg, Zn, O, and Cu elements. The dark-grey dendritic structure (indicated by white arrow) is evenly distributed in the base phase of 50Mg-25Zn-24Fe-0.5Cu-0.5Co, 70Mg-25Zn-4Fe-0.5Cu-0.5Co, and 90Mg-5Zn-4Fe-0.5Cu-0.5Co alloys, which indicates the formation of the $MgZn_2$, Fe and Cu phase. The inter-dendritic structure (shown by black arrow) or base alloys was a solid solution, consisting of the Mg and MgO phases.

Table 1. High entropy properties of Mg-Zn-Fe-Cu-Co alloys

Alloys	ΔHm (kJ/mol)	ΔSm (J/K mol)	ΔG	δ
20Mg20Zn20Fe20Cu20Co	2.321	12.6	6.70	12.463
50Mg25Zn24Fe0.5Cu0.5Co	5.116	6.83	1.37	16.130
70Mg25Zn4Fe0.5Cu0.5Co	-0.27	4.04	-13.5	17.527
90Mg5Zn4Fe0.5Cu0.5Co	0.820	1.80	2.06	18.490

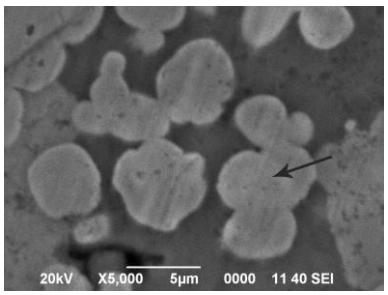

(a)

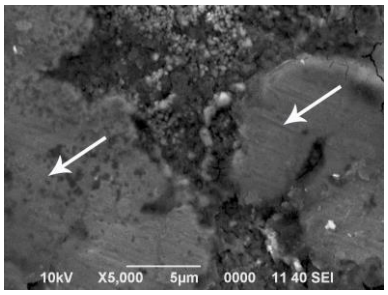

(b)

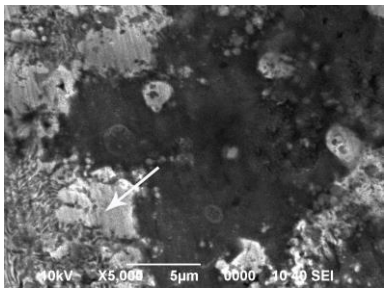

(c)

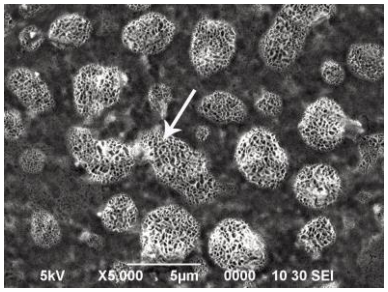

(d)

Figure 3. SEM images of Mg-Zn-Fe-Cu-Co alloys: (a) 20Mg-20Zn-20Fe-20Cu-20Co; (b) 50Mg-25Zn-24Fe-0.5Cu-0.5Co; (c) 70Mg-25Zn-4Fe-0.5Cu-0.5Co; (d) 90Mg-5Zn-4Fe-0.5Cu-0.5Co; and (e) pure Mg

The MgO peak was higher because magnesium tends to react with oxygen, and MgO was the main oxide phase in the magnesium matrix. MgO differs from other combining elements in that MgO was formed at the grain boundaries, whereas MgO is uniformly distributed in the Mg matrix. The presence of MgO can increase the hardness of magnesium and can also stimulate the formation of pores on the surface of Mg which is very useful for implant applications that can be damaged [26].

3.2. Mechanical Properties of Mg-Zn-Fe-Cu-Co Alloys

The densities and hardness of Mg-Zn-Fe-Cu-Co alloys were shown in Fig 4(a), and Fig 4(b) respectively. Mg-Zn-Fe-Cu-Co alloys exhibited medium densities (3.057 $g.cm^{-3}$ – 1.711 $g.cm^{-3}$) and medium hardness (286 HV-81 HV), as can be seen in Table 2. The density of the alloy decreases with the increase of magnesium addition, while the densities increase with increasing Zn content in alloys [19],[27]. The shape of the Zn and Mg grains is relatively the same as the spherical shape and the particle size of Mg is larger than Zn. When Zn and Mg are combined, the smaller Zn particles will fill the space between the larger Mg particles. Therefore, the Zn particles will diffuse into Mg [28]. Decreasing the density can also be caused by the lack of pressure during the compaction process [27]. The actual density (gradient line) is lower than theoretical density (black line) as shown in Fig. 4 (a), where the greatest loss was found in 90Mg-5Zn-4Fe-0.5Cu-0.5Co alloys by 36%. The low density was caused by the presence of oxides and porosity which occurs on samples during the sintering process in addition to the imperfections sintering process [29].

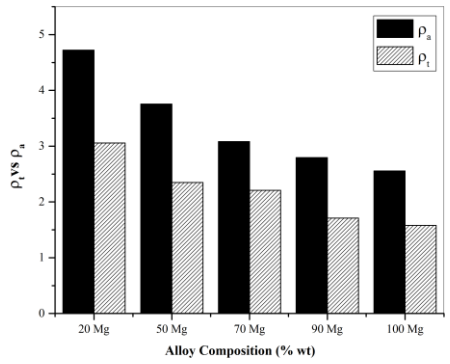

(a)

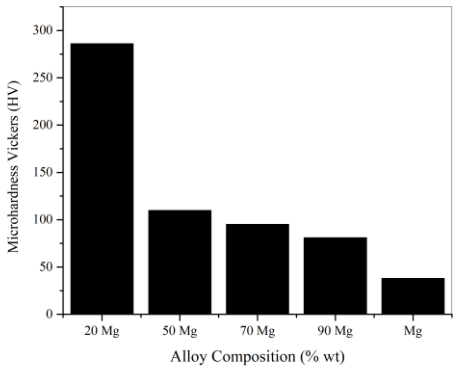

(b)

Figure 4. (a) Actual density vs theoretical density of Mg-Zn-Fe-Cu-Co, (b) microhardness of Mg-Zn-Fe-Cu-Co and (c) presence pores on surface of 20Mg-20Zn-20Fe-20Cu-20Co alloy

Figure 4(b) clearly shows that a similar pattern of behavior in hardness result was obtained. This reduction in hardness over 20Mg-20Zn-20Fe-20Cu-20Co may be a result of the increasing magnesium content in the alloy. The high hardness of 20Mg-20Zn-20Fe-20Cu-20Co (286.08 HV) is due to the presence of an intermetallic phase and high density [30]. The Co-Fe phase is an intermetallic phase present at the grain boundaries of the 20Mg-20Zn-20Fe-20Cu-20Co alloy, resulting from the predominance of Co and Fe elements. It is also believed that the $MgZn_2$ phase as laves phase in the matrix makes the alloy harder and brittle [25]. The hardness of Mg-Zn-Fe-Cu-Co is promising for candidate ureteral application because it was similar to the AZ31 alloy (120-132 HV) and ZK60 alloy (~100 HV) that have been reported in previous studies [2], [31]-[32].

Table 2. Density and micro-hardness properties of Mg-Zn-Fe-Cu-Co alloys at room temperature

Alloy	ρ_{theory} ($g.cm^{-3}$)	ρ_{actual} ($g.cm^{-3}$)	% Porosity	Micro-Hardness (HV)
20Mg	4.721	3.057	35	286.06
50Mg	3.756	2.347	37	109.78
70Mg	3.082	2.207	28	95
90Mg	2.795	1.711	39	80.98
Mg	2.557	1.581	38	37.9

4. CONCLUSIONS

In the current study, biomaterial high entropy Mg-Zn-Fe-Cu-Co alloy was effectively produced by powder metallurgy route, while mechanical and morphological properties were intensively explored. The following are the finding of the study. Mg-Zn-Fe-Cu-Co alloys were designed by utilizing the strategy of equiatomic ratio and high entropy of mixing. The alloys were essentially multiphase and crystalline. An alloy of 20Mg-20Zn-20Fe-20Cu-20Co has consisted of the HCP phase and cubic phase.

The physical and mechanical properties of Mg-Zn-Fe-Cu-Co were influenced by the magnesium content in the matrix alloys. The presence of pores gave poor results in terms of compaction and the sintering process. Mg-Zn-Fe-Cu-Co alloys have a medium hardness between 286.06 HV and 80.98 HV, while the densities of alloys were moderate between 3.057 $g.cm^{-3}$ and 1.71 $g.cm^{-3}$. It is believed that solid solution strengthening and intermetallic strengthening were the main strengthening mechanics of the alloys.

Based on the results it is concluded that high entropy is a promising method for the processing of Mg elements. Moreover, the 20Mg-20Zn-20Fe-20Cu-20Co alloy having ideal mechanical properties that meet the minimum requirements for high entropy alloys. But further developments still need to be done, such as optimization of the sintering temperature in the process of making high entropy alloys and controlling the oxidation of magnesium alloys using the powder metallurgy method, so that the formation of the alloy surface becomes smoother.

ACKNOWLEDGEMENT

This project is supported by Research Center for Metallurgy and Materials, Indonesian Institute of Science and Departement of Metallurgical Engineering, Bandung Institute of Technology.

REFERENCES

[1] R. Kurniawan, "Profile of patients with urinary tract stone at urology departement of Soetomo general hospital Surabaya in january 2016-december 2016," *Indonesian Journal of Urology*, vol. 27, no 1, pp. 22-25, 2020. Doi: 10.32421/juri.v27i1.506.

[2] S. Zhang, Y. Bi, J. Li, Z. Wang, J. Yan, J. Song, H. Sheng, H. Guo, and Y. Li, "Biodegradation behavior of magnesium and ZK60 alloy in artificial urine and rat models," *Bioact. Mater.*, vol. 2, no. 2, pp. 53–62, 2017. Doi :10.1016/j.bioactmat.2017.03.004.

[3] Z. Ma, M. Gao, D. Na, Y. Li, L. Tan, and K. Yang, "Study on a biodegradable antibacterial Fe-Mn-C-Cu alloy as urinary implant material," *Mater. Sci. Eng. C*, vol. 103, no. May, 2019. Doi:10.1016/j.msec.2019.05.003.

[4] J. Y. Lock, E. Wyatt, S. Upadhyayula, A. Whall, V. Nuñez, V. I. Vullev, and H. Liu, "Degradation and antibacterial properties of magnesium alloys in artificial urine for potential resorbable ureteral stent applications," *J. Biomed. Mater. Res. - Part A*, vol. 102, no. 3, pp. 781–792, 2014. Doi : 10.1002/jbm.a.34741.

[5] D. Tie, H. Liu, R. Guan, P. Holt-Torres, Y. Liu, Y. Wang, and N. Hort, "In vivo assessment of biodegradable magnesium alloy ureteral stents in a pig model," *Acta Biomater.*, vol. 116, pp. 415–425, 2020. Doi: 10.1016/j.actbio.2020.09.023.

[6] K. Zhang, H. Cui, H. Jiang, Y. Hao, R. Long, Q. Ma, and H. Zhang, "The current status and applications of ureteral stents,"

Int. J. Clin. Exp. Med., vol. 13, no. 4, pp. 2122–2133, 2020.

[7] F. Soria, E. Morcillo, A. Serrano, A. Budia, I. Fernández, T. Fernández-Aparicio, and F. M. Sanchez-Margallo, "Evaluation of a new design of antireflux-biodegradable ureteral stent in animal model," *Urology*, vol. 115, pp. 59–64, 2018. Doi: 10.1016/j.urology.2018.02.004.

[8] X. Ma, Y. Xiao, H. Xu, K. Lei, and M. Lang, "Preparation, degradation and in vitro release of ciprofloxacin-eluting ureteral stents for potential antibacterial application," *Mater. Sci. Eng. C*, vol. 66, pp. 92–99, 2016. Doi : 10.1016/j.msec.2016.04.072.

[9] Y. Chen, J. Dou, H. Yu, and C. Chen, "Degradable magnesium-based alloys for biomedical applications: The role of critical alloying elements," *J. Biomater. Appl.*, vol. 33, no. 10, pp. 1348–1372, 2019. Doi :10.1177/0885328219834656.

[10] D. Orlov, G. Raab, T. T. Lamark, M. Popov, and Y. Estrin, "Improvement of mechanical properties of magnesium alloy ZK60 by integrated extrusion and equal channel angular pressing," *Acta Mater.*, vol. 59, no. 1, pp. 375–385, 2011. Doi:10.1016/j.actamat.2010.09.043.

[11] W. Yu, Z. Liu, H. He, N. Cheng, and X. Li, "Microstructure and mechanical properties of ZK60-Yb magnesium alloys," *Mater. Sci. Eng. A*, vol. 478, no. 1–2, pp. 101–107, 2008. Doi :10.1016/j.msea.2007.09.027.

[12] S. Champagne, E. Mostaed, F. Safizadeh, E. Ghali, M. Vedani, and H. Hermawan, "In vitro degradation of absorbable zinc alloys in artificial urine," *Materials (Basel).*, vol. 12, no. 2, pp. 1–13, 2019. Doi :10.3390/ma12020295.

[13] Y. Ding, C. Wen, P. Hodgson, and Y. Li, "Effects of alloying elements on the corrosion behavior and biocompatibility of biodegradable magnesium alloys: A review," *J. Mater. Chem. B*, vol. 2, no. 14, pp. 1912–1933, 2014. Doi :10.1039/C3TB21746A.

[14] S. Agarwal, J. Curtin, B. Duffy, and S. Jaiswal, "Biodegradable magnesium alloys for orthopaedic applications: A review on corrosion, biocompatibility and surface modifications," *Mater. Sci. Eng. C*, vol. 68, pp. 948–963, 2016. Doi : 10.1016/j.msec.2016.06.020.

[15] S. K. Jaganathan, E. Supriyanto, S. Murugesan, A. Balaji, and M. K. Asokan, "Biomaterials in cardiovascular research: Applications and clinical implications," *Biomed Res. Int.*, vol. 2014, 2014. Doi : 10.1155/2014/459465.

[16] G. Senopati, C. Sutowo, F. Rokhmanto, I. Kartika, and B. Suharno, "Microstructure , mechanical properties , and corrosion resistance of Ti-6Mo-6Nb-xSn alloys for biomedical application," vol. 988, pp. 175–181, 2020. Doi : 10.4028/www.scientific.net/MSF.988.175.

[17] M. Todai, T. Nagase, T. Hori, A. Matsugaki, A. Sekita, and T. Nakano, "Novel TiNbTaZrMo high-entropy alloys for metallic biomaterials," *Scr. Mater.*, vol. 129, pp. 65–68, 2017. Doi : 10.1016/j.scriptamat.2016.10.028.

[18] V. Geanta, I. Voiculescu, P. Vizureanu, and A. Victor Sandu, "High entropy alloys for medical applications," *Eng. Steels High Entropy-Alloys*, pp. 4–12, 2020. Doi : 10.5772/intechopen.89318.

[19] R. Li, J. Gao, and K. Fa, "Study to microstructure and mechanical properties of Mg containing high entropy alloys," *Mater. Sci. Forum*, vol. 650, pp. 265–271, 2010. Doi : 10.4028/www.scientific.net/MSF.650.265.

[20] Y. J. Zhou, Y. Zhang, Y. L. Wang, and G. L. Chen, "Solid solution alloys of AlCoCrFeNi Tix with excellent room-temperature mechanical properties," *Appl. Phys. Lett.*, vol. 90, no. 18, 2007. Doi :10.1063/1.2734517.

[21] A. Kumar and M. Gupta, "An insight into evolution of light weight high entropy alloys: A review," *Metals (Basel).*, vol. 6, no. 9, 2016. Doi : 10.3390/met6090199.

[22] N. Sharma, G. Singh, P. Sharma, and A. Singla, "Development of Mg-Alloy by powder metallurgy method and its characterization," *Powder Metall. Met. Ceram.*, vol. 58, no. 3–4, pp. 163–169, 2019. Doi : 10.1007/s11106-019-00060-5.

[23] A. R. Miedema, P. F. de Châtel, and F. R. de Boer, "Cohesion in alloys - fundamentals of a semi-empirical model," *Phys. B+C*, vol. 100, no. 1, pp. 1–28, 1980. Doi :10.1016/0378-4363(80)90054-6.

[24] L. A. Dreval, M. A. Turchanin, P. G. Agraval, and Y. Du, "Cu–Fe–Co system: Verification of the high-temperature phase equilibria and thermodynamic modeling of the low-temperature phase relations involving ordered phase," *Powder Metall. Met. Ceram.*, vol. 56, no. 9–10, pp. 546–

555, 2018. Doi :10.1007/s11106-018-9927-7.
[25] J. Nei, K. Young, S. O. Salley, and K. Y. S. Ng, "Determination of C14/C15 phase abundance in laves phase alloys," *Mater. Chem. Phys.*, vol. 136, no. 2–3, pp. 520–527, 2012. Doi : 10.1016/j.matchemphys.2012.07.020.
[26] Y. Chen, Z. Feng, and W. Zhang, "Effect of MgO content on mechanical properties of directionally solidified pure magnesium," *Mater. Res.*, vol. 24, no. 2, 2021. Doi : 10.1590/1980-5373-MR-2020-0469.
[27] M. Y. Kolawole, J. O. Aweda, F. Iqbal, A. Ali, and S. Abdulkareem, "Mechanical properties of powder metallurgy processed biodegradable Zn-based alloy for biomedical application," *Int. J. Mater. Metall. Eng.*, vol. 13, no. 12, pp. 558–563, 2019. Doi :10.5281/zenodo.3593236.
[28] J. Yu, J. Wang, Q. Li, J. Shang, J. Cao, and X. Sun, "Effect of Zn on microstructures and properties of Mg-Zn alloys prepared by powder metallurgy method," *Rare Met. Mater. Eng.*, vol. 45, no. 11, pp. 2757–2762, 2016. Doi : 10.1016/S1875-5372(17)30035-8.
[29] E. M. Salleh, H. Zuhailawati, S. Ramakrishnan, and M. A. H. Gepreel, "A statistical prediction of density and hardness of biodegradable mechanically alloyed Mg-Zn alloy using fractional factorial design," *J. Alloys Compd.*, vol. 644, pp. 476–484, 2015. Doi :10.1016/j.jallcom.2015.04.090.
[30] G. Tosun and M. Kurt, "The porosity, microstructure, and hardness of Al-Mg composites reinforced with micro particle SiC/Al2O3 produced using powder metallurgy," *Compos. Part B Eng.*, vol. 174, p. 106965, 2019. Doi : 10.1016/j.compositesb.2019.106965.
[31] S. A. Torbati-Sarraf and T. G. Langdon, "Properties of a ZK60 magnesium alloy processed by high-pressure torsion," *J. Alloys Compd.*, vol. 613, pp. 357–363, 2014. Doi : 10.1016/j.jallcom.2014.06.056.
[32] J. Xu, X. Wang, M. Shirooyeh, G. Xing, D. Shan, B. Guo, and T. G. Langdon, "Microhardness, microstructure and tensile behavior of an AZ31 magnesium alloy processed by high-pressure torsion," *J. Mater. Sci.*, vol. 50, no. 22, pp. 7424–7436, 2015. Doi :10.1007/s10853-015-9300-x.